The Role of Whitecap Bubbles in Air–Sea Heat and Moisture Exchange

EDGAR L ANDREAS

U.S. Army Cold Regions Research and Engineering Laboratory, Hanover, New Hampshire

EDWARD C. MONAHAN

Department of Marine Sciences, University of Connecticut, Groton, Connecticut

(Manuscript received 6 May 1998, in final form 15 April 1999)

ABSTRACT

In high winds, the sea surface is no longer simply connected. Whitecap bubbles and sea spray provide additional surfaces that may enhance the transfer of any quantity normally exchanged at the air–sea interface. This paper investigates the role that the air bubbles in whitecaps play in the air–sea exchange of sensible and latent heat. Bubble spectra published in the literature suggest that an upper bound on the volume flux of bubbles per unit surface area in Stage A whitecaps is 3.8×10^{-2} m^3 m^{-2} s^{-1}. This estimate, a knowledge of whitecap coverage as a function of wind speed, and microphysical arguments lead to estimates of the sensible (Q_{bS}) and latent (Q_{bL}) heat fluxes carried across the sea surface by air cycled through whitecap bubbles. Because Q_{bS} and Q_{bL} scale as do the usual turbulent or interfacial fluxes of sensible and latent heat, these bubble fluxes can be represented simply as multiplicative factors f_S and f_L, respectively, that modulate the 10-m bulk transfer coefficients for sensible (C_{H10}) and latent (C_{E10}) heat. Computations show, however, that even the upper bounds on the bubble heat fluxes are too small to be measured. For 10-m wind speeds up to 20 m s^{-1}, f_S and f_L are always between 1.00 and 1.01. For a 10-m wind speed of 40 m s^{-1}, f_S and f_L are still less than 1.05. Consequently, for wind speeds up to 40 m s^{-1}—a range over which it should be safe to extrapolate the models of sea surface physics used here—the near-surface air heated and moistened in whitecap bubbles seems incapable of contributing measurably to air–sea heat and moisture transfer.

1. Introduction

On a wave-roughened, whitecapped sea surface, processes in the near-surface air mirror processes in the near-surface water. Both fluids are multiphase. Above the interface, the air hosts spray droplets; below the interface, the water is filled with air bubbles. The spray and the bubbles effectively increase the ocean's surface area so that surface is no longer simply connected (Kraus and Businger 1994). Any constituent normally transferred across the air–sea interface may now experience enhanced transfer mediated by both the spray and the bubbles.

While many scientists in the last 25 years have studied the role that sea spray plays in the air–sea transfer of latent and sensible heat (e.g., Bortkovskii 1973, 1987; Borisenkov 1974; Wu 1974; Ling and Kao 1976; Wang and Street 1978a, 1978b; Ling et al. 1980; Mestayer and Lefauconnier 1988; Mestayer et al. 1989, 1996; Fairall et al. 1990, 1994; Rouault et al. 1991; Andreas 1992; Ling 1993; Edson and Fairall 1994; Andreas et al. 1995; Edson et al. 1996), we know of no comparable work on the role that bubbles play in air–sea heat transfer. Therefore, here we make what, we believe, is the first estimate of how effective bubbles are in carrying heat and moisture across the air–sea interface.

Our concept is simple: Breaking waves entrain near-surface air that is heated and moistened in whitecap bubbles. When these bubbles rise again to the surface and burst, the expelled air carries sensible and latent heat across the air–sea interface. We estimate, first, the rate at which these bubble rise to the surface and, then, the amount of heating and moistening of the air within them.

2. Whitecap bubble concentrations and volume fluxes

To determine how the bubbles produced by breaking waves contribute to the air–sea exchange of heat and moisture, we need two pieces of information. One is the flux of bubbles back to the sea surface within a whitecap; the other is the average whitecap coverage as a function of wind speed. Combining these two quantities

Corresponding author address: Dr. Edgar L Andreas, U.S. Army Cold Regions Research and Engineering Laboratory, 72 Lyme Road, Hanover, NH 03755-1290.
E-mail: eandreas@crrel.usace.army.mil

yields the spatially averaged flux of bubbles to the sea surface. We begin with the whitecap coverage.

Monahan (1989, 1993) identifies two visible stages in whitecap development—Stage A and Stage B whitecaps. Spilling wave crests and a dense concentration of bubbles with a very broad size spectrum characterize Stage A whitecaps. Stage B whitecaps are the diffuse, dissipating remains of Stage A whitecaps. As such, the bubbles in the plumes beneath Stage B whitecaps are more widely distributed and have a narrower size spectrum, but the surface fraction covered by Stage B whitecaps is far larger than for Stage A whitecaps.

The fraction of the ocean's surface covered by both Stage A (W_A) and Stage B (W_B) whitecaps is roughly proportional to the third power of the wind speed at 10 m, U_{10}. Monahan and O'Muircheartaigh (1980) find

$$W_B = 3.84 \times 10^{-6}\, U_{10}^{3.41}, \tag{2.1}$$

while Fig. 2, line A1, in Monahan (1989) (cf. Monahan et al. 1988; Smith et al. 1990) gives

$$W_A = 3.16 \times 10^{-7}\, U_{10}^{3.2}. \tag{2.2}$$

In both (2.1) and (2.2), W_A and W_B are fractions of the sea surface covered by Stage A or Stage B whitecaps for U_{10} in meters per second.

Next we look at the size-dependent concentration of bubbles beneath a spilling wave crest: that is, at bubbles within the α plume beneath a Stage A whitecap (e.g., Fig. 1 in Monahan and Lu 1990). Figure 1 depicts various estimates of this concentration spectrum, where $\partial C/\partial R$ is the number of bubbles per cubic meter of seawater per micrometer increment in bubble radius R.

Curve A in Fig. 1 comes from Monahan (1988a, 1989) and derives, in some measure, from estimates of the rate at which bursting whitecap bubbles produce sea spray droplets (Monahan 1988b). The dashed portion of curve A represents a power-law extrapolation to larger radii for the purposes of this study.

Curve B is the published version of the bubble concentration spectrum that Deane (1997) obtained for individual breaking waves in the surf zone. Here we focus on the two power-law segments, one for each of the bubble size domains shown in Deane's Fig. 7.

During the review of this manuscript, however, G. B. Deane (1998, personal communication) alerted us that his published bubble spectrum had been plotted incorrectly; plotted bubble radii need to be divided by 2. Curve B′ in Fig. 1 is Deane's (1997) published spectrum adjusted according to this advice. Notice, in the 175–1000 μm range of bubble radii, curve B′ now falls closer to curve A than does curve B.

Curve C is from Carey et al. (1993) and represents the peak bubble concentration spectrum obtained in saltwater, tipping-trough experiments. We have omitted in Fig. 1 the small-bubble portion of this spectrum, while the dashed line represents a modest extrapolation of the curve to bubble radii beyond 700 μm.

Finally, curve D is the large-radius end of the oft-cited Medwin and Breitz (1989) bubble spectrum, which we have shifted up in amplitude to coincide with the maximum values depicted in their Fig. 6. These values were obtained in the open ocean immediately after a breaker occurred.

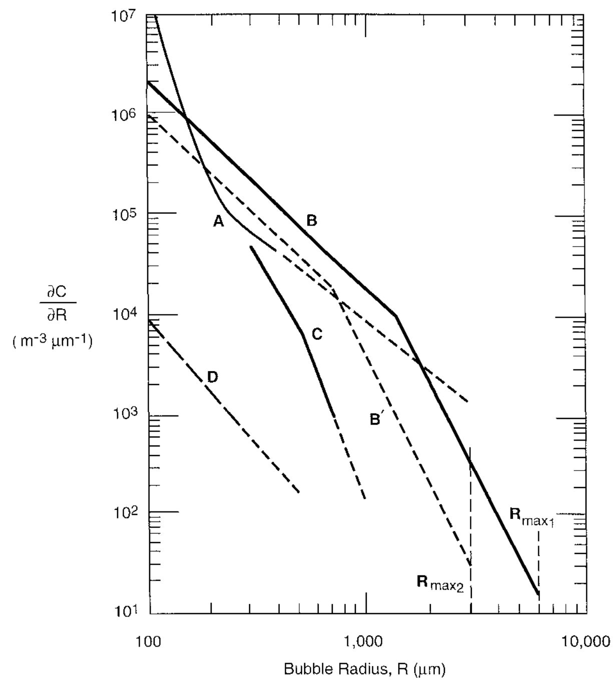

FIG. 1. Bubble concentration spectra beneath breaking waves. The units on $\partial C/\partial R$ are number of bubbles per cubic meter per micrometer increment in bubble radius. Spectrum A, from Monahan (1988a, 1989), is inferred from the sea spray generation rate. Spectrum B, from Deane (1997), is for waves breaking in the surf zone. Spectrum B′ is a corrected version of spectrum B (see text). Spectrum C, from Carey et al. (1993), is from tipping-trough experiments. Spectrum D, from Medwin and Breitz (1989), is acoustically determined under breaking waves in the open ocean. See the text for other details.

To place an upper bound on bubble effects, we adopt Deane's (1997) published bubble concentration spectrum, curve B in Fig. 1, for the calculations that follow. Note that over much of the relevant large-bubble domain this spectrum agrees within a factor of 4 with the spectrum from Monahan (1988a, 1989), curve A.

From Deane's (1997) spectrum, we calculate the aggregate bubble volume flux to the sea surface associated with the α bubble plume found beneath a Stage A whitecap. This air volume flux is

$$V_A = \frac{4\pi}{3} \int_0^{R_{\max}} R^3 u(R) \frac{\partial C}{\partial R}\, dR, \tag{2.3}$$

which gives V_A in cubic meters of air per square meter of surface per second. Here, also, $u(R)$ is the terminal rise velocity of ''dirty'' bubbles. We obtained this variable from Fig. 7.3 in Clift et al. (1978) for the larger bubbles and from Thorpe (1982) for the smaller bubbles. Carrying out the integration in (2.3) for radii up to

6 mm, the $R_{\max_1}$ shown in Fig. 1, yields an aggregate bubble volume flux in a Stage A whitecap of

$$V_A = 3.8 \times 10^{-2} \text{ m}^3 \text{ m}^{-2} \text{ s}^{-1}. \tag{2.4}$$

When we use Deane's revised spectrum, curve B′ in Fig. 1, the integration for radii up to 3 mm, $R_{\max_2}$ in Fig. 1, yields

$$V_A = 3.9 \times 10^{-3} \text{ m}^3 \text{ m}^{-2} \text{ s}^{-1}. \tag{2.5}$$

It is also informative to calculate the void fraction υ_α associated with these α bubble plumes. This value derives from

$$\upsilon_\alpha = \frac{4\pi}{3} \int_0^{R_{\max}} R^3 \frac{\partial C}{\partial R}\, dR, \tag{2.6}$$

which is the aggregate volume of the bubbles within a unit volume of seawater. If the upper bound on R is again taken as $R_{\max_1} = 6$ mm, the void fraction computed from Deane's (1997) published bubble spectrum is 22.5%. This value agrees quite well with the maximum void fraction that Melville et al. (1993) report from their laboratory wave channel experiments. On the other hand, if we take the upper bound on R as 3 mm, $R_{\max_2}$ in Fig. 1, Deane's published bubble spectrum yields $\upsilon_\alpha = 15.9\%$, which agrees very well with the peak void fraction that Carey et al. (1993) find in their tipping-trough experiments. If we had used this smaller upper bound on R in evaluating (2.3), the resulting aggregate bubble volume flux would have been $V_A = 2.5 \times 10^{-2}$ m^3 m^{-2} s^{-1} instead of (2.4). Finally, when we use Deane's revised bubble spectrum (curve B′) and integrate (2.6) to $R_{\max_2} = 3$ mm, we obtain a void fraction of only 2.8%.

Not all bubbles in the α plume beneath a Stage A whitecap reach the sea surface before the associated breaking wave ceases to entrain additional air, that is, before this whitecap transforms into a Stage B whitecap (i.e., a dissipating foam patch). Using the bubble concentration spectrum under Stage B whitecaps (Monahan 1988a, 1989), we followed arguments like those above to estimate the aggregate bubble volume flux at the sea surface in Stage B whitecaps. That flux,

$$V_B = 1.4 \times 10^{-7} \text{ m}^3 \text{ m}^{-2} \text{ s}^{-1}, \tag{2.7}$$

computed for bubbles with radii less than 150 μm, is several orders of magnitude smaller than the flux from Stage A whitecaps, (2.4) or (2.5).

For Deane's (1997) published bubble spectrum, the area-averaged bubble volume flux from Stage A whitecaps as a function of wind speed is simply

$$V_A W_A = 1.2 \times 10^{-8}\ U_{10}^{3.2}, \tag{2.8}$$

if $R_{\max}$ is 6 mm and

$$V_A W_A = 7.9 \times 10^{-9}\ U_{10}^{3.2} \tag{2.9}$$

if $R_{\max}$ is 3 mm. For Deane's (1997) revised α-plume bubble spectrum, the area-averaged bubble volume flux for Stage A whitecaps is only

$$V_A W_A = 1.2 \times 10^{-9}\ U_{10}^{3.2}. \tag{2.10}$$

The area-averaged bubble flux from Stage B whitecaps is

$$V_B W_B = 5.4 \times 10^{-13}\ U_{10}^{3.41}. \tag{2.11}$$

Because the bubble flux sustained by Stage A whitecaps is orders of magnitude larger than the flux for Stage B whitecaps at all realistic wind speeds, we focus henceforth only on Stage A whitecaps. Also, we adopt (2.8) rather than (2.9) or (2.10) for use in our subsequent calculations. Although (2.8) derives from curve B in Fig. 1, which G. B. Deane (1998, personal communication) says was plotted incorrectly when it was published, curve B does yield a void fraction that agrees well with other independent estimates of this quantity. Curve B′, our corrected version of curve B, on the other hand, implies a void fraction that seems too small in the light of independent observations. Thus, (2.8) should provide, at the very least, a reasonable upper bound on the direct bubble contribution to the air–sea heat and moisture fluxes.

3. Mathematical formulation of the bubble heat fluxes

To evaluate whether bubbles can sustain appreciable fluxes of sensible and latent heat, we must ultimately compare the bubble fluxes with the usual turbulent or interfacial fluxes of sensible (H_S) and latent (H_L) heat. These interfacial fluxes can be modeled as

$$H_S = -\rho c_p u_* t_* = \rho c_p C_{H10} U_{10}(T_w - T_{10}), \tag{3.1a}$$

$$H_L = -\rho L_v u_* q_* = \rho L_v C_{E10} U_{10}(q_w - q_{10}). \tag{3.1b}$$

Here ρ is the air density; c_p the specific heat of air at constant pressure; L_v the latent heat of vaporization; T_w the sea surface temperature; q_w the specific humidity of air in saturation with seawater of temperature T_w; U_{10}, again, the wind speed at 10 m; and T_{10} and q_{10} the air temperature and specific humidity at 10 m.

Also in (3.1), the friction velocity u_* is related to the momentum flux or surface stress by

$$\tau = \rho u_*^2 = \rho C_{D10} U_{10}^2. \tag{3.2}$$

The flux scales t_* and q_* in (3.1) relate the sensible and latent heat fluxes, respectively, to the average profiles of temperature and specific humidity:

$$T(z) = T_w + \frac{t_*}{k}[\ln(z/z_T) - \psi_h(z/L)], \tag{3.3a}$$

$$q(z) = q_w + \frac{q_*}{k}[\ln(z/z_q) - \psi_h(z/L)], \tag{3.3b}$$

where z is the height; k (=0.4) the von Kármán constant; z_T and z_q roughness lengths for temperature and humidity; and ψ_h an empirical profile correction that depends on the stability parameter z/L, where L is the Obukhov length.

Finally in (3.1) and (3.2), C_{H10}, C_{E10}, and C_{D10} are dimensionless bulk transfer coefficients for sensible heat, latent heat, and momentum fluxes that we will say more about later.

When a wave crest breaks or spills, it engulfs near-surface air that, say, has temperature T_h. This air gets distributed into bubbles that range in radius from 10 μm to 10 mm. These bubbles then quickly heat or cool to the temperature of the surrounding water.

Since bubble-mediated exchange—if relevant at all—will be important only for high winds, we can assume that the temperature of the water around the bubbles is T_w, the sea surface temperature. In light winds, the sea surface can have a thin cool skin or warm layer (e.g., Schluessel et al. 1990; Fairall et al. 1996a) with a temperature that is a few tenths of a degree different from that of the bulk water underneath. In higher winds, however, breaking waves and whitecaps destroy these thin surface films. For example, from extensive measurements along a transect across the equator in the Atlantic Ocean, Donlon and Robinson (1997) find that, for winds exceeding 10 m s^{-1}, the radiometrically determined surface temperature and the water temperature at 5.5-m depth agree within 0.1°C, the resolution of their measurement system. Many others corroborate that wind mixing homogenizes the near-surface ocean to depths of several meters (e.g., Price et al. 1986; Moum 1990). Hence, for our purposes, bubbles encounter only seawater of temperature very near T_w.

Andreas's (1990) study of sea spray droplets coming to equilibrium in air provides insight into the thermal evolution of bubbles. All spray droplets with radii of 500 μm or less reach thermal equilibrium in air in less than 10 s. Because the bubbles can be an order of magnitude larger than these spray droplets but have 3000 times less heat capacity than spray droplets of the same radius, all bubbles will easily reach temperature equilibrium within a second. Farmer and Gemmrich (1996, their Fig. A1) confirm that even bubbles with radii of 10 mm need only about a second to reach temperature equilibrium.

The life cycle of a whitecap bubble includes a plunge to depths of decimeters to meters followed by a gravitational rise to the sea surface before effervescent bursting in a whitecap (e.g., Monahan et al. 1982; Thorpe 1986). Woolf (1993) suggests that the maximum rise velocity for clean or dirty bubbles of radius 1 mm or greater is 0.25 m s^{-1} in 20°C seawater. Smaller bubbles rise more slowly. Consequently, bubbles of the sizes that we are considering need to be submerged only about 25 cm for the air in them to reach T_w. Since spilling or plunging breakers can carry bubbles much deeper, the air in most bursting whitecap bubbles will have temperature T_w.

In effect, breaking waves entrain air at temperature T_h and expel that air at temperature T_w. Consequently, the sensible heat flux across the air–sea interface carried by whitecap bubbles is

$$Q_{bS} = W_A V_A \rho c_p (T_w - T_h). \tag{3.4}$$

The height h from which the air is entrained is still uncertain. Koga's (1982) work suggests that spilling breakers entrain air that is within 1 cm of the sea surface. Plunging breakers, on the other hand, could engulf air a meter above the surface. In other words, T_h could reasonably be the temperature of the air between 1 cm and 1 m above the sea surface.

Using (3.3a), we can model T_h in terms of T_{10}. That is,

$$T_h = T_{10} + \frac{t_*}{k}[\ln(h/10) - \psi_h(h/L) + \psi_h(10/L)], \tag{3.5}$$

where h must be in meters. From (3.1a) and (3.2), we also obtain

$$t_* = \frac{-C_{H10}(T_w - T_{10})}{C_{D10}^{1/2}}. \tag{3.6}$$

Substituting (3.6) and (3.5) into (3.4) yields

$$\begin{aligned} Q_{bS} = {} & W_A V_A \rho c_p \\ & \times \left\{1 + \frac{C_{H10}}{k C_{D10}^{1/2}}[\ln(h/10) - \psi_h(h/L) + \psi_h(10/L)]\right\} \\ & \times (T_w - T_{10}). \end{aligned} \tag{3.7}$$

This now represents the sensible heat flux supported by the bubbles and parameterized by the standard 10-m air temperature T_{10} rather than T_h. The air entrainment height h is still a free parameter.

Whitecap bubbles also transport latent heat across the air–sea interface. The air entrapped by breaking waves starts with the specific humidity of the near-surface air, say q_h, where, as above, h denotes the height from which the air is entrained.

Estimating the specific humidity in a bubble is a bit more complicated than estimating the bubble's temperature. The salinity of the surrounding water, the bubble's curvature, and the additional pressure a bubble encounters on its excursion to depths of 1–3 m all affect the vapor pressure within the bubble. Again, the microphysical model that Andreas (1989, 1990) developed to investigate the evolution of spray droplets yields some insights into the probable range of humidities within bubbles.

The vapor pressure (e_R) at the interior surface of a bubble of radius R in water of temperature T_w and salinity S can be written as (Pruppacher and Klett 1978, pp. 80 ff., 139 ff.; Andreas 1989)

$$\ln\left[\frac{e_R(T_w, S, P)}{e_{sat}(T_w, P)}\right] = -\left[\frac{2M_w\sigma_s}{R_g(T_w + 273.15)\rho_w R} + \nu m M_w \Phi_s\right]. \tag{3.8}$$

Here, $e_{sat}(T_w, P)$ is the saturation vapor pressure over a planar surface of pure water at pressure P, M_w ($=18.0160 \times 10^{-3}$ kg mol^{-1}) is the molecular weight

TABLE 1. Terms in Eq. (3.8) for whitecap bubbles of various radii, as computed using the microphysical model described in Andreas (1989). Water temperature is taken as 20°C; and salinity, as 34 psu.

Radius, R	Curvature term	Solute term	e_R/e_{sat}
10 μm	-1.095×10^{-4}	-0.0201	0.9800
20 μm	-5.476×10^{-5}	-0.0201	0.9801
50 μm	-2.190×10^{-5}	-0.0201	0.9801
100 μm	-1.095×10^{-5}	-0.0201	0.9801
200 μm	-5.476×10^{-6}	-0.0201	0.9801
500 μm	-2.190×10^{-6}	-0.0201	0.9801
1 mm	-1.095×10^{-6}	-0.0201	0.9801
2 mm	-5.476×10^{-7}	-0.0201	0.9801
5 mm	-2.190×10^{-7}	-0.0201	0.9801
10 mm	-1.095×10^{-7}	-0.0201	0.9801

of water, R_g (=8.314 41 J mol^{-1} K^{-1}) is the universal gas constant, ρ_w, is the water density, $\nu = 2$ for saltwater, and

$$m = \frac{S}{M_s(1 - S)}, \tag{3.9}$$

where M_s (=58.443×10^{-3} kg mol^{-1}) is the molecular weight of NaCl, and S must be the fractional salinity. Andreas (1989) gives functions for the surface tension of seawater, σ_s, and for the practical osmotic coefficient Φ_s.

The first term on the right-hand side of (3.8) is the curvature term: The vapor pressure inside a bubble is less than that over a planar surface because the bubble is spherical. The second term on the right is the solute term: The salt in the water also decreases the vapor pressure within the bubble compared to pure water. Table 1 lists values of the curvature term, the solute term, and e_R/e_{sat} for typical ocean conditions and for the range of bubble sizes that we feel is relevant. Clearly, the curvature term is negligible in this size range; while the effects of the salt in depressing vapor pressure can be estimated by the usual equation for the pressure of water vapor in equilibrium with saline water (e.g., Roll 1965, p. 262),

$$\frac{e_R(T_w, S, P)}{e_{sat}(T_w, P)} = 1 - 5.37 \times 10^{-4} S, \tag{3.10}$$

where S is in practical salinity units here.

Pressure affects $e_{sat}(T_w, P)$. Buck (1981) reports

$$e_{sat}(T_w, P) = 6.1121(1.0007 + 3.46 \times 10^{-6} P) \times \exp\left(\frac{17.502T_w}{240.97 + T_w}\right), \tag{3.11}$$

which gives e_{sat} in millibars for P in millibars and T_w in degrees Celsius. Although Buck admittedly develops this formula to treat pressure in the atmosphere, which is typically 1040 mb or less, we should be relatively safe extrapolating (3.11) to slightly higher pressures, especially since the constant multiplying pressure is so small. Leifer (1995) estimates that, for ocean depths between the surface and 3 m, the pressure within whitecap bubbles with radius 10 μm is 1.5–2 atmospheres. Substituting 2000 mb in (3.11), we see that such pressure increases e_{sat} over its value at normal sea level pressure, 1000 mb, by about 0.3%—a negligible effect. Leifer also shows that bubbles at shallower depths or with larger radii have far smaller interior pressure. Hence, for the near-surface bubbles with radii larger than 10 μm, which are our main interest, we can ignore the effects of water pressure on e_R.

As a result, given enough time, the interior of a whitecap bubble will reach specific humidity q_w, the same humidity that air in saturation with the sea surface has. That is,

$$q_w = \frac{\rho_{\upsilon,sat}}{\rho_d + \rho_{\upsilon,sat}}, \tag{3.12}$$

where

$$\rho_{\upsilon,sat} = \frac{100M_w e_{sat}(T_w, P)(1 - 5.37 \times 10^{-4} S)}{R_g(T_w + 273.15)} \tag{3.13}$$

is the density of water vapor in equilibrium with the sea surface and ρ_d is the density of dry air at temperature T_w and pressure P. In (3.13), e_{sat} comes from (3.11), T_w is in degrees Celsius, S is in practical salinity units, and the 100 provides a vapor density in kilograms per cubic meter when vapor pressure is in millibars.

The question then becomes: How much time does a bubble need to reach moisture equilibrium with the surrounding seawater? Again, Andreas's (1989, 1990) microphysical model of sea spray droplets provides order-of-magnitude estimates. In air at 20°C and with a relative humidity of 80%, a seawater droplet with salinity 34 psu and initial radius 500 μm—the largest droplets Andreas studies—evaporates to radius 341 μm in 3400 s (Andreas 1990). In other words, in 3400 s, that spray droplet exchanges 3.6×10^{-7} kg of water vapor.

Suppose the seawater is also at 20°C and that a breaking wave has engulfed near-surface air with 80% relative humidity. According to (3.10), a 500-μm bubble formed from that entrained air must reach a relative humidity of 98.2% to be in moisture equilibrium with the water around it. That is, at 20°C and 80% relative humidity, that 500-μm bubble initially contains 7.2×10^{-12} kg of water vapor but needs to contain 8.9×10^{-12} kg to be in equilibrium. Consequently, we must estimate how much time that bubble would take to extract 1.7×10^{-12} kg of water vapor from the seawater surrounding it. If a 500-μm spray droplet takes 3400 s to give up 3.6×10^{-7} kg of water vapor, we predict a similarly sized air bubble will require about 0.02 s to take up five orders of magnitude less water vapor.

Bubbles at the large end of the range that we are considering, 6 mm—over 10 times larger than this 500-μm bubble—will take considerably longer to reach moisture equilibrium. We can estimate how long by simply adapting Farmer and Gemmrich's (1996) analysis for temperature diffusion in a bubble to vapor diffusion. The only change necessary is replacing the molecular diffusivity of heat in air, D, with the molecular diffusivity of water vapor in air, D_v. Since D_v is about 20% larger than D, the timescale for a bubble to reach vapor equilibrium is actually shorter than the scale for temperature equilibrium. From Fig. A1 in Farmer and Gemmrich, we estimate that bubbles with 6-mm radius reach vapor equilibrium in less than 0.5 s. Again, this equilibration time is shorter than a bubble's lifetime. As a result, it seems very likely that most bursting whitecap bubbles will be saturated with water vapor and, thus, have specific humidity q_w.

Having gone through these estimates, we can now simply write down an expression for the latent heat that whitecap bubbles transport across the air–sea interface that is analogous to (3.4),

$$Q_{bL} = W_A V_A \rho L_v (q_w - q_h). \tag{3.14}$$

As we did with temperature, we can express q_h in terms of the reference specific humidity at 10 m, q_{10}. The steps are exactly the same as in (3.5)–(3.7) except we use (3.1b) and (3.3b) instead of (3.1a) and (3.3a), respectively. Thus, we simply write down the result for the bubble latent heat flux:

$$Q_{bL} = W_A V_A \rho L_v \times \left\{1 + \frac{C_{E10}}{kC_{D10}^{1/2}}[\ln(h/10) - \psi_h(h/L) + \psi_h(10/L)]\right\} \times (q_w - q_{10}). \tag{3.15}$$

Coincidentally, (3.7) and (3.15) look quite similar to the respective bulk-aerodynamic expressions for the turbulent or interfacial fluxes of sensible (H_S) and latent (H_L) heat, (3.1). Combining (3.7) and (3.1a) and (3.15) and (3.1b), we obtain expressions for the total (i.e., interfacial plus bubbles) sensible ($H_{S,T}$) and latent ($H_{L,T}$) heat fluxes at the air–sea interface:

$$H_{S,T} = \rho c_p C_{H10} U_{10} \left\langle 1 + \frac{W_A V_A}{U_{10} C_{H10}} \left\{1 + \frac{C_{H10}}{kC_{D10}^{1/2}}\left[\ln\left(\frac{h}{10}\right) - \psi_h\left(\frac{h}{L}\right) + \psi_h\left(\frac{10}{L}\right)\right]\right\}\right\rangle (T_w - T_{10}), \tag{3.16a}$$

$$H_{L,T} = \rho L_v C_{E10} U_{10} \left\langle 1 + \frac{W_A V_A}{U_{10} C_{E10}} \left\{1 + \frac{C_{E10}}{kC_{D10}^{1/2}}\left[\ln\left(\frac{h}{10}\right) - \psi_h\left(\frac{h}{L}\right) + \psi_h\left(\frac{10}{L}\right)\right]\right\}\right\rangle (q_w - q_{10}). \tag{3.16b}$$

That is, the bubble fluxes simply enhance the usual bulk transfer coefficients with wind-speed-dependent modification factors that we can readily calculate. Call these factors f_S and f_L, where from (2.8) and (3.16)

$$f_S = 1 + \frac{1.2 \times 10^{-8} U_{10}^{2.2}}{C_{H10}} \times \left\{1 + \frac{C_{H10}}{kC_{D10}^{1/2}}\left[\ln\left(\frac{h}{10}\right) - \psi_h\left(\frac{h}{L}\right) + \psi_h\left(\frac{10}{L}\right)\right]\right\}, \tag{3.17a}$$

$$f_L = 1 + \frac{1.2 \times 10^{-8} U_{10}^{2.2}}{C_{E10}} \times \left\{1 + \frac{C_{E10}}{kC_{D10}^{1/2}}\left[\ln\left(\frac{h}{10}\right) - \psi_h\left(\frac{h}{L}\right) + \psi_h\left(\frac{10}{L}\right)\right]\right\}. \tag{3.17b}$$

Here, again, U_{10} must be in meters per second and h must be in meters.

To evaluate C_{H10} and C_{E10} in (3.16) and (3.17), we use the COARE bulk flux algorithm (Fairall et al. 1996b). This gives the bulk transfer coefficients as functions of the observation height z (=10 m), stability, and the roughness lengths for momentum (z_0), temperature (z_T), and humidity (z_q):

$$C_{H10} = \frac{k^2}{[\ln(z/z_0) - \psi_m(z/L)][\ln(z/z_T) - \psi_h(z/L)]}, \tag{3.18a}$$

$$C_{E10} = \frac{k^2}{[\ln(z/z_0) - \psi_m(z/L)][\ln(z/z_q) - \psi_h(z/L)]}. \tag{3.18b}$$

Here ψ_m is another empirical stability correction.

We will ultimately see that f_S and f_L are basically one except in very high winds, where $h/L \approx 10/L \approx z/L \approx 0$ and $\psi_m \approx \psi_h \approx 0$. Hence, in the ensuing calculations, we ignore the ψ terms in (3.17) and (3.18). Consequently, C_{D10}, C_{H10}, and C_{E10} depend only on z_0, z_T, and z_q. The COARE algorithm predicts z_T and z_q. We estimate z_0 via the neutral-stability drag coefficient evaluated at 10 m, C_{DN10} (Large and Pond 1981):

$$10^3 C_{DN10} = \begin{cases} 1.20 & \text{for } 4 \le U_{10} \le 11 \text{ m s}^{-1} \quad (3.19a) \\ 0.49 + 0.065U_{10} & \text{for } 11 \text{ m s}^{-1} \le U_{10}. \quad (3.19b) \end{cases}$$

This relates monotonically to z_0 through

$$z_0 = 10 \exp(-kC_{DN10}^{-1/2}), \tag{3.20}$$

which gives z_0 in meters.

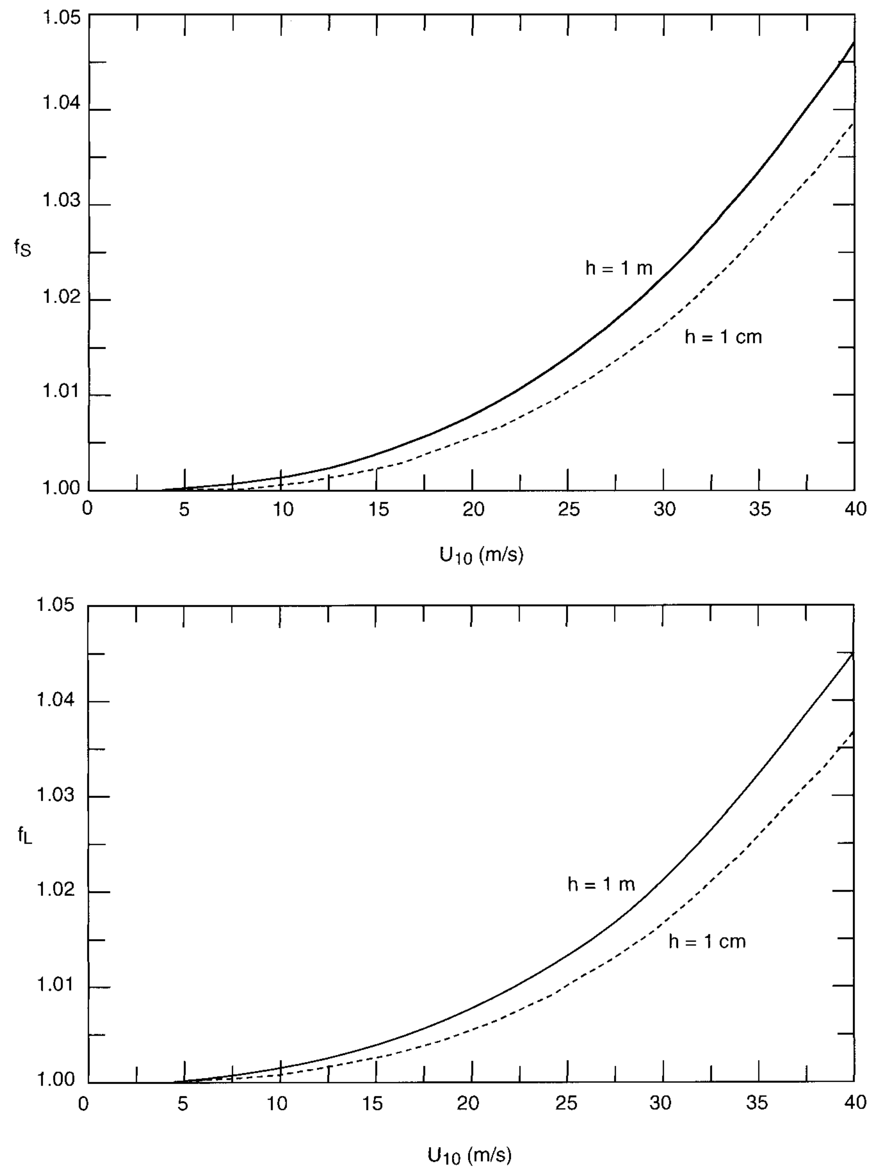

FIG. 2. The modification factors f_S and f_L, (3.17), that account for how whitecap bubbles influence the usual bulk transfer coefficients for sensible and latent heat in (3.16); U_{10} is the 10-m wind speed, and h is the height from which bubble air is entrained. Stability is assumed to be near neutral.

4. Results

With the COARE algorithm and our modifications to it, it is easy to compute the bubble modification factors f_S and f_L in (3.17) in a spreadsheet. Figure 2 plots these factors for 10-m wind speeds up to 40 m s^{-1} and for large and small values of the air entrainment height *h*. Despite the fact that both f_S and f_L increase faster than the square of the wind speed [see (3.17)], for wind speeds up to 40 m s^{-1}—the maximum wind speed to which we dare to extrapolate the relationships developed in the last two sections—bubbles seem to have very little direct influence on air–sea heat and moisture transfer. At a 10-m wind speed of 40 m s^{-1}, our model suggests that, as an upper bound, bubble transport augments the usual interfacial fluxes by only 4%–5%. Such a small effect is within the experimental uncertainty of C_{H10} and C_{E10} values and is, thus, currently undetectable, even with the best instruments for measuring the air–sea heat fluxes.

If we had used Deane's revised bubble spectrum instead of his presumably erroneous published spectrum in our analysis—that is, if we had used (2.10) instead of (2.8) in (3.16)—the estimated bubble enhancement would be only about 0.5% for a 40 m s^{-1} wind.

The influence of the height from which the bubble air is entrained—that is, h—is clear in Fig. 2 and from (3.4) and (3.14). The magnitudes of the bubble fluxes increase with h. Physically, this result just acknowledges that the magnitudes of the sea–air temperature and humidity differences increase with h. For small h, T_h is very near T_w and q_h is very near q_w; bubbles formed from air this close to the surface, thus, have little potential for altering the heat and moisture content of the near-surface air. As h increases, though, T_h and T_w tend to diverge, as do q_h and q_w. Bubbles are therefore entraining air farther from equilibrium with the seawater and can influence it more.

Although bubbles are plentiful in Stage A whitecaps and, in fact, take up a significant fraction of the volume in the α plume under a whitecap, they simply do not have a lot of heat-carrying capacity. First, the air in them does not have the thermal capacity to transport much sensible heat across the air–sea interface. Second, because bubbles have no mechanism to concentrate the water vapor they carry, they are no more efficient in exchanging moisture than the sea surface itself is.

Still, whitecaps begin proliferating at wind speeds of 4–6 m s^{-1} (Monahan 1971) and, hence, begin cycling near-surface air through the near-surface ocean. It is, therefore, conceivable that bubble-mediated heat exchange is inextricably mixed with strict interfacial exchange in our current parameterizations for C_{H10} and C_{E10}. Although the z_T and z_q parameterization in the COARE algorithm (Fairall et al. 1996b) derives from the Liu et al. (1979) surface renewal model, which is based on strict interfacial exchange, that parameterization is ''tuned'' with data. Because bubble and interfacial effects would be inseparable in those data because they scale the same, the current parameterizations for C_{H10} and C_{E10} in low-to-moderate winds may implicitly include bubble effects. After all, we have shown that transfer processes within bubbles are fast enough to effectively increase the ocean's surface area.

The focus of our study, however, is high winds, where we have explicitly parameterized the effects of bubble-mediated exchange on the bulk transfer coefficients. Since the Liu et al. (1979) model contains no such parameterization, z_T and z_q values for high winds that are deduced from it cannot be modeling all the bubble-mediated exchange, although they may be modeling some bubble contributions for lower wind speeds because of the data-based tuning. Thus, in effect, our flux equations (3.16) largely separate interfacial and bubble-mediated heat exchange for high wind speeds but, perhaps, not for lower wind speeds. The point is, of course, academic rather than practical because we have found these parameterized bubble effects to be unmeasurably small for wind speeds up to at least 40 m s^{-1}.

5. Conclusions

The source of the anomalously large heat fluxes that seem necessary to generate and maintain hurricanes (e.g., Emanuel 1995; Smith 1997) is a mystery. Many have looked to sea spray for this source, but Emanuel (1995) believes spray cannot explain it. Rather, he (K. A. Emanuel 1997, personal communication) thinks whitecap bubbles have more potential to augment the air–sea heat and moisture fluxes. Our purpose here was to investigate this hypothesis.

We therefore reviewed Stage A and Stage B whitecap bubble spectra available in the literature and estimated the volume fluxes per unit area from these. Stage A whitecaps support a bubble flux that appears to be no larger than 3.8×10^{-2} m^3 m^{-2} s^{-1}; Stage B whitecaps support a bubble flux of 1.4×10^{-7} m^3 m^{-2} s^{-1}. Using published relations for whitecap coverage as a function of 10-m wind speed, we saw that Stage A whitecaps cycle roughly four orders of magnitude more air through the near-surface ocean than do Stage B whitecaps for a given wind speed. We thus focused our analysis on the role of Stage A whitecaps.

Relying on the microphysical sea spray model that Andreas (1989, 1990) describes and on Farmer and Gemmrich's (1996) evaluation of bubble equilibration times, we argued that the sensible and latent heat fluxes that bubbles foster scale as do the interfacial or turbulent fluxes of sensible and latent heat. That is, the total (interfacial plus bubbles) air–sea sensible and latent heat fluxes can be parameterized as

$$H_{S,T} = \rho c_p C_{H10} f_S U_{10}(T_w - T_{10}), \qquad (5.1a)$$

$$H_{L,T} = \rho L_v C_{E10} f_L U_{10}(q_w - q_{10}), \qquad (5.1b)$$

where f_S and f_L are wind-speed-dependent bubble modification factors. Our estimates of f_S and f_L, however, suggest that these are little different from one for U_{10} up to 20 m s^{-1} and are no more than 5% larger than one for $U_{10} = 40$ m s^{-1}. We, therefore, conclude that, for wind speeds within the range of current sea surface physics models and observable with current surface-based instruments, whitecap bubbles have negligible direct influence on the air–sea exchange of latent and sensible heat.

This conclusion leaves us again with sea spray as the most likely source of the enhanced air–sea heat and moisture fluxes in hurricane-strength winds. Fairall et al. (1994) already inferred from their model of the tropical cyclone boundary layer that sea spray can play this role. More recently, Andreas and DeCosmo (1999) extracted a measurable sea spray signal for wind speeds as low as 15 m s^{-1} from DeCosmo's (1991) eddy-correlation measurements of sensible and latent heat fluxes. Having here found that bubbles are inefficient vehicles for transporting heat and moisture across the air–sea interface, we must continue studying spray's role in this process.

Acknowledgments. We thank Kerry Emanuel for pointing out the necessity of this study, Chris Fairall for supplying the FORTRAN code for the COARE algorithm, Ira Leifer for helpful suggestions, Grant Deane for reviewing the manuscript, and an anonymous reviewer for urging us to make our analysis more precise. The Office of Naval Research supported this work through Contracts N0001498MP30029 and N0001499MP30043.

REFERENCES

Andreas, E. L, 1989: Thermal and size evolution of sea spray droplets. CRREL Rep. 89-11, U.S. Army Cold Regions Research and Engineering Laboratory, Hanover, NH, 37 pp. [NTIS AD-A210484.]

——, 1990: Time constants for the evolution of sea spray droplets. *Tellus,* **42B,** 481–497.

——, 1992: Sea spray and the turbulent air–sea heat fluxes. *J. Geophys. Res.,* **97,** 11 429–11 441.

——, and J. DeCosmo, 1999: Sea spray production and influence on air–sea heat and moisture fluxes over the open ocean. *Air–Sea Fluxes: Momentum, Heat, and Mass Exchange,* G. L. Geernaert, Ed., Kluwer, in press.

——, J. B. Edson, E. C. Monahan, M. P. Rouault, and S. D. Smith, 1995: The spray contribution to net evaporation from the sea: A review of recent progress. *Bound.-Layer Meteor.,* **72,** 3–52.

Borisenkov, E. P., 1974: Some mechanisms of atmosphere–ocean interaction under stormy weather conditions. *Probl. Arctic Antarct.,* **43–44,** 73–83.

Bortkovskii, R. S., 1973: On the mechanism of interaction between the ocean and the atmosphere during a storm. *Fluid Mech.—Sov. Res.,* **2,** 87–94.

——, 1987: *Air–Sea Exchange of Heat and Moisture during Storms.* D. Reidel, 194 pp.

Buck, A. L., 1981: New equations for computing vapor pressure and enhancement factor. *J. Appl. Meteor.,* **20,** 1527–1532.

Carey, W. M., J. W. Fitzgerald, E. C. Monahan, and Q. Wang, 1993: Measurements of the sound produced by a tipping trough with fresh and salt water. *J. Acoust. Soc. Amer.,* **93,** 3178–3192.

Clift, R., J. R. Grace, and M. E. Weber, 1978: *Bubbles, Drops, and Particles.* Academic Press, 380 pp.

Deane, G. B., 1997: Sound generation and air entrainment by breaking waves in the surf zone. *J. Acoust. Soc. Amer.,* **102,** 2671–2689.

DeCosmo, J., 1991: Air–sea exchange of momentum, heat and water vapor over whitecap sea states. Ph.D. dissertation, University of Washington, 212 pp. [Available from UMI Dissertation Services, P.O. Box 1346, Ann Arbor, MI 48106-1346.]

Donlon, C. J., and I. S. Robinson, 1997: Observations of the oceanic thermal skin in the Atlantic Ocean. *J. Geophys. Res.,* **102,** 18 585–18 606.

Edson, J. B., and C. W. Fairall, 1994: Spray droplet modeling: 1. Lagrangian model simulation of the turbulent transport of evaporating droplets. *J. Geophys. Res.,* **99,** 25 295–25 311.

——, S. Anquentin, P. G. Mestayer, and J. F. Sini, 1996: Spray droplet modeling: 2. An interactive Eulerian–Lagrangian model of evaporating spray droplets. *J. Geophys. Res.,* **101,** 1279–1293.

Emanuel, K. A., 1995: Sensitivity of tropical cyclones to surface exchange coefficients and a revised steady-state model incorporating eye dynamics. *J. Atmos. Sci.,* **52,** 3969–3976.

Fairall, C. W., J. B. Edson, and M. A. Miller, 1990: Heat fluxes, whitecaps, and sea spray. *Surface Waves and Fluxes,* G. L. Geernaert and W. J. Plant, Eds., Vol. 1., Kluwer, 173–208.

——, J. D. Kepert, and G. J. Holland, 1994: The effect of sea spray on surface energy transports over the ocean. *Global Atmos. Ocean Syst.,* **2,** 121–142.

——, E. F. Bradley, J. S. Godfrey, G. A. Wick, J. B. Edson, and G. S. Young, 1996a: Cool-skin and warm-layer effects on sea surface temperature. *J. Geophys. Res.,* **101,** 1295–1308.

——, ——, D. P. Rogers, J. B. Edson, and G. S. Young, 1996b: Bulk parameterization of air–sea fluxes for Tropical Ocean–Global Atmosphere Coupled-Ocean Atmosphere Response Experiment. *J. Geophys. Res.,* **101,** 3747–3764.

Farmer, D. M., and J. R. Gemmrich, 1996: Measurements of temperature fluctuations in breaking surface waves. *J. Phys. Oceanogr.,* **26,** 816–825.

Koga, M., 1982: Bubble entrainment in breaking wind waves. *Tellus,* **34,** 481–489.

Kraus, E. B., and J. A. Businger, 1994: *Atmosphere–Ocean Interaction.* 2d ed. Oxford University Press, 362 pp.

Large, W. G., and S. Pond, 1981: Open ocean momentum flux measurements in moderate to strong winds. *J. Phys. Oceanogr.,* **11,** 324–336.

Leifer, I. S., 1995: A validation study of bubble mediated air–sea gas transfer modeling. Ph.D. dissertation, Georgia Institute of Technology, 218 pp. [Available from UMI Dissertation Services, P.O. Box 1346, Ann Arbor, MI 48106-1346.]

Ling, S. C., 1993: Effect of breaking waves on the transport of heat and water vapor fluxes from the ocean. *J. Phys. Oceanogr.,* **23,** 2360–2372.

——, and T. W. Kao, 1976: Parameterization of the moisture and heat transfer process over the ocean under whitecap sea states. *J. Phys. Oceanogr.,* **6,** 306–315.

——, ——, and A. I. Saad, 1980: Microdroplets and transport of moisture from ocean. *Proc. ASCE, J. Eng. Mech. Div.,* **106,** 1327–1339.

Liu, W. T., K. B. Katsaros, and J. A. Businger, 1979: Bulk parameterization of air–sea exchanges of heat and water vapor including the molecular constraints at the interface. *J. Atmos. Sci.,* **36,** 1722–1735.

Medwin, H., and N. D. Breitz, 1989: Ambient and transient bubble spectral densities in quiescent seas and under spilling breakers. *J. Geophys. Res.,* **94,** 12 751–12 759.

Melville, W. K., M. R. Loewen, and E. Lamarre, 1993: Bubbles, noise and breaking waves: A review of laboratory experiments. *Natural Physical Sources of Underwater Sound,* B. R. Kerman, Ed., Kluwer, 483–501.

Mestayer, P. G., and C. Lefauconnier, 1988: Spray droplet generation, transport, and evaporation in a wind wave tunnel during the Humidity Exchange over the Sea Experiments in the Simulation Tunnel. *J. Geophys. Res.,* **93,** 572–586.

——, J. B. Edson, C. W. Fairall, S. E. Larsen, and D. E. Spiel, 1989: Turbulent transport and evaporation of droplets generated at an air–water interface. *Turbulent Shear Flows 6,* J.-C. André, J. Cousteix, F. Durst, B. E. Launder, F. W. Schmidt, and J. H. Whitelaw, Eds. Springer-Verlag, 129–147.

——, A. M. J. Van Eijx, G. de Leeuw, and B. Tranchant, 1996: Numerical simulation of the dynamics of sea spray over the waves. *J. Geophys. Res.,* **101,** 20 771–20 797.

Monahan, E. C., 1971: Oceanic whitecaps. *J. Phys. Oceanogr.,* **1,** 139–144.

——, 1988a: Near-surface bubble concentration and oceanic whitecap coverage. Preprints, *Seventh Conf. Ocean–Atmosphere Interaction,* Anaheim, CA, Amer. Meteor. Soc., 178–181.

——, 1988b: Whitecap coverage as a remotely monitorable indication of the rate of bubble injection into the oceanic mixed layer. *Sea Surface Sound,* B. R. Kerman, Ed., Kluwer, 85–96.

——, 1989: From the laboratory tank to the global ocean. *The Climate and Health Implications of Bubble-Mediated Sea–Air Exchange,* E. C. Monahan and M. A. Van Patten, Eds., Connecticut Sea Grant Program, 43–63.

——, 1993: Occurrence and evolution of acoustically relevant subsurface bubble plumes and their associated, remotely monitorable, surface whitecaps. *Natural Physical Sources of Underwater Sound,* B. R. Kerman, Ed., Kluwer, 503–517.

——, and I. Ó Muircheartaigh, 1980: Optimal power-law description of oceanic whitecap coverage dependence on wind speed. *J. Phys. Oceanogr.,* **10,** 2094–2099.

——, and M. Lu, 1990: Acoustically relevant bubble assemblages and their dependence on meteorological parameters. *IEEE J. Oceanic Eng.,* **15,** 340–349.

——, K. L. Davidson, and D. E. Spiel, 1982: Whitecap aerosol productivity deduced from simulation tank measurements. *J. Geophys. Res.,* **87,** 8898–8904.
——, M. B. Wilson, and D. K. Woolf, 1988: HEXMAX whitecap climatology: Foam crest coverage in the North Sea, 16 October–23 November 1986. *Proc. NATO Advanced Workshop on Humidity Exchange over the Sea Main Experiment (HEXMAX): Analysis and Interpretation,* Dellenhove, Epe, Netherlands, NATO, 243 pp. [Available from Dept. of Atmospheric Sciences, AK-40, University of Washington, Seattle, WA 98195.]
Moum, J. N., 1990: Profiler measurements of vertical velocity fluctuations in the ocean. *J. Atmos. Oceanic Technol.,* **7,** 323–333.
Price, J. F., R. A. Weller, and R. Pinkel, 1986: Diurnal cycling: Observations and models of the upper ocean response to diurnal heating, cooling, and wind mixing. *J. Geophys. Res.,* **91,** 8411–8427.
Pruppacher, H. R., and J. D. Klett, 1978: *Microphysics of Clouds and Precipitation.* D. Reidel, 714 pp.
Roll, H. U., 1965: *Physics of the Marine Atmosphere.* Academic Press, 426 pp.
Rouault, M. P., P. G. Mestayer, and R. Schiestel, 1991: A model of evaporating spray droplet dispersion. *J. Geophys. Res.,* **96,** 7181–7200.
Schluessel, P., W. J. Emery, H. Grassl, and T. Mammen, 1990: On the bulk-skin temperature difference and its impact on satellite remote sensing of sea surface temperature. *J. Geophys. Res.,* **95,** 13 341–13 356.
Smith, R. K., 1997: On the theory of CISK. *Quart. J. Roy. Meteor. Soc.,* **123,** 407–418.
Smith, S. D., K. B. Katsaros, W. A. Oost, and P. G. Mestayer, 1990: Two major experiments in the Humidity Exchange over the Sea (HEXOS) program. *Bull. Amer. Meteor. Soc.,* **71,** 161–172.
Thorpe, S. A., 1982: On the clouds of bubbles formed by breaking wind waves in deep water, and their role in air-sea gas transfer. *Philos. Trans. Roy. Soc. London,* **A304,** 155–210.
——, 1986: Measurements with an automatically recording inverted echo sounder; ARIES and the bubble clouds. *J. Phys. Oceanogr.,* **16,** 1462–1478.
Wang, C. S., and R. L. Street, 1978a: Measurements of spray at an air–water interface. *Dyn. Atmos. Oceans,* **2,** 141–152.
——, and ——, 1978b: Transfer across an air–water interface at high wind speeds: The effect of spray. *J. Geophys. Res.,* **83,** 2959–2969.
Woolf, D. K., 1993: Bubbles and the air–sea transfer velocity of gases. *Atmos.–Ocean,* **31,** 517–540.
Wu, J., 1974: Evaporation due to spray. *J. Geophys. Res.,* **79,** 4107–4109.